UDC 621
DOI https://doi.org/10.32782/2663-5941/2026.3.2/21

Klymenko V.M.
https://orcid.org/0009-0005-9532-6744
National Technical University «Kharkiv Polytechnic Institute»

Avdieieva O.P.
https://orcid.org/0000-0002-9358-4265
National Technical University «Kharkiv Polytechnic Institute»

Usatiy O.P.
https://orcid.org/0000-0002-8568-5007
National Technical University «Kharkiv Polytechnic Institute»

MULTI-CRITERIA OPTIMIZATION OF GAS TURBINE BLADE MATERIALS BASED ON LIFE CYCLE ASSESSMENT: INTEGRATING ECONOMIC, ENVIRONMENTAL, AND PERFORMANCE METRICS

Material selection for first-stage gas turbine blades has historically prioritized high-temperature mechanical performance and first cost, while underrepresenting life-cycle environmental burdens, end-of-life (EOL) value, and time-dependent degradation effects that accumulate over decades of operation. This creates systematic biases in design decisions under carbon pricing and circular-economy policies. This study develops an integrated multi-criteria decision framework to identify Pareto-optimal turbine-blade materials by jointly minimizing life-cycle cost (LCC) and global warming potential (GWP), while maximizing operational efficiency and power density under realistic degradation trajectories. We formulate a cradle-to-grave life cycle assessment (LCA) and net-present-value (NPV) life cycle cost model with an explicit coupling to degradation-driven efficiency decay. The operational efficiency is modeled as depend on temperature, stress, and material-specific kinetics. Environmental impacts follow ISO 14040/14044 and account for production, operation, and EOL recycling credits. The multi-objective problem is solved using NSGA-III with feasibility constraints on stress, temperature margin, creep rate, and oxidation kinetics. For a representative 400 MW combined-cycle-class turbine (7000 h/yr, 25 yr design life), operational fuel-related impacts dominated both LCC and GWP across candidates (typically 65–78% of discounted LCC). Incorporating degradation increased discounted operational costs by 15–23% compared with static-efficiency assumptions, altering rankings and expanding the Pareto set. High-recyclability options (Inconel 718, Ti-6Al-4V) achieved an 8–12% reduction in total GWP versus low-recyclability single-crystal alternatives under equivalent boundary conditions, while premium single-crystal CMSX-4 became favorable only in high-temperature, baseload-dominant scenarios where 2–3% efficiency gains amortize over lifetime. Coupling LCC–LCA with degradation is necessary for robust material selection under carbon pricing and circular-economy constraints. The proposed framework produces stakeholder-specific Pareto-optimal recommendations and is extensible to other high-temperature energy systems.

Keywords: *Life cycle assessment, Multi-criteria optimization, Turbine blade materials, Pareto optimization, Circular economy*

Formulation of the problem. Gas turbines remain a critical technology for electricity systems due to their high-power density, dispatchability, and compatibility with combined-cycle configurations. At the same time, the sector operates under intensifying constraints: higher turbine inlet temperatures are pursued to improve thermal efficiency, while carbon pricing and sustainability policies require quantifiable reductions of life-cycle greenhouse gas (GHG) emissions. In this context, the first-stage blade is an archetypal "extreme" component: it experiences high centrifugal stresses, aggressive oxidation/corrosion environments, and thermal gradients, all while directly influencing aerodynamic performance and thus fuel consumption over decades.

Conventional blade-material selection is typically framed as a materials-science optimization problem: maximize creep strength and oxidation resistance,

ensure manufacturability, and meet a cost target based largely on upfront procurement and processing. However, a blade material is also an economic and environmental decision. Small differences in achievable efficiency, and especially in efficiency retention under degradation, can dominate discounted fuel costs and operational emissions. Likewise, end-of-life routes–scrap value, closed-loop recycling, and substitution of virgin alloy production–can yield meaningful credits within a cradle-to-grave boundary, yet are rarely integrated explicitly into early material-choice decisions.

This creates an important methodological issue: when selection ignores time-dependent degradation and circularity, the optimization landscape is distorted. Materials that deliver high initial efficiency but degrade more rapidly may appear favorable under static assumptions, while durable and recyclable candidates may be undervalued. As carbon prices increase and circular-economy requirements tighten, such distortions translate into non-trivial financial and compliance risks.

Analysis of recent research and publications. Nickel-based superalloys (e.g., Inconel series, René alloys) and single-crystal (SX) superalloys (e.g., CMSX families) have been the workhorse for hot-section blades due to their creep resistance at elevated temperature, microstructural stability, and compatibility with protective coatings and thermal barrier systems. Traditional screening emphasizes properties such as high-temperature yield/creep strength, oxidation resistance, thermal fatigue resistance, and manufacturability (casting route, heat-treatment windows, defect tolerance). Foundational reviews and monographs [1, 2] summarize the evolution from equiaxed to directionally solidified and SX alloys, including the role of γ/γ′ microstructures, refractory-element additions, and coating interactions [1; 2]. Nevertheless, these approaches usually treat performance as a quasi-static attribute measured at beginning-of-life or under short test durations.

Life cycle assessment (LCA), standardized by ISO 14040/14044, provides a structured method to quantify environmental impacts across production, operation, and end-of-life stages. In energy technologies, LCA is routinely applied to fuels, power plants, and major infrastructure, but component-level LCA for high-temperature alloys is less common and often limited by data granularity. The literature documents [3-7] that operation-phase impacts can dominate for fossil-based generation, while manufacturing may become relatively more important as grids decarbonize. Environmental product declarations (EPDs) and background databases provide emission factors for metals, but alloy-specific pathways, scrap fractions, and recycling substitution assumptions can change results materially [3, 4, 5, 6, 7].

Multi-criteria decision-making (MCDM) methods (e.g., TOPSIS, VIKOR, PROMETHEE) and evolutionary multi-objective optimization (e.g., NSGA-II/III, MOPSO) have been widely used in engineering design to navigate trade-offs among cost, performance, and sustainability metrics. In material selection specifically, MCDM methods provide transparent ranking but can be sensitive to normalization and subjective weights, while Pareto-based evolutionary algorithms provide sets of non-dominated solutions and allow stakeholder-specific ex post selection [8, 9, 10, 11]. However, many studies treat the evaluation functions as static and do not incorporate time-dependent degradation that affects both economics and emissions through efficiency.

Blade degradation arises from multiple coupled mechanisms: creep, oxidation, hot corrosion, and thermal fatigue. Creep is often captured using constitutive relations such as Norton power-law creep and damage mechanics extensions (e.g., Kachanov–Rabotnov) to represent tertiary creep and rupture. Oxidation and corrosion kinetics may be approximated by parabolic rate laws with Arrhenius temperature dependence. When integrated into reliability and maintenance planning, degradation models support life prediction and inspection intervals; yet their explicit integration into LCC–LCA-driven material selection is not standard practice [12, 13, 14].

To the best of our knowledge, no study has integrated (i) cradle-to-grave LCA with explicit recycling credits, (ii) discounted life cycle costing, and (iii) time-dependent degradation-driven efficiency decay in a unified multi-objective optimization framework for gas turbine blade material selection. In particular, the coupling between degradation and both economic and environmental operational metrics is frequently simplified or neglected, and recyclability is rarely treated as a first-class optimization variable rather than a qualitative discussion point.

Task statement.

This work aims to:

1. develop an integrated LCC–LCA model for turbine blade materials under a cradle-to-grave boundary;

2. incorporate time-dependent degradation (creep and corrosion/oxidation) into efficiency and cost/emissions accounting;

3. quantify trade-offs among economic, environmental, and performance objectives;

4. generate Pareto-optimal material portfolios/choices using NSGA-III;

5. demonstrate the method on an industrial gas turbine case study.

Outline of the main material of the study. Mathematical framework.

Life cycle cost (LCC) model. For a material choice , the discounted life cycle cost is:

$$LCC(m) = C_{\text{initial}}(m) + C_{\text{operation}}(m) + C_{\text{maintenance}}(m) - C_{\text{EOL}}(m). \quad (1)$$

Initial costs. Let $M_{\text{blade}}(\text{m}) = \rho(\text{m})V_{\text{blade}}$ be blade mass based on density ρ and blade volume V_{blade} .

$$C_{\text{initial}}(m) = M_{\text{blade}}(m)\left[P_{\text{mat}}(m)\left(1 + w_{\text{scrap}}\right) + C_{\text{mfg}}(m)\right], \quad (2)$$

where P_{mat} is material price, w_{scrap} is a scrap fraction in manufacturing, and C_{mfg} aggregates machining, coating, heat treatment, and inspection.

Operational costs (NPV). Degradation affects efficiency and thus fuel cost over time:

$$C_{\text{operation}}(\text{m}) = \sum_{t=1}^{T} \frac{" P_{\text{fuel}}(m,t) H_{\text{annual}} P_{\text{fuel}}(t)}{(1+r)^t}, \quad (3)$$

where T is life in years, H_{annual} annual operating hours, P_{fuel} fuel price trajectory, and r the discount rate.

We relate incremental fuel penalty to efficiency loss (relative to a baseline):

$$\Delta P_{\text{fuel}}(\text{m},\text{t}) = P_{\text{rated}}\left(\frac{1}{\eta(m,t)} - \frac{1}{\eta_{\text{base}}}\right) D\text{F}(\text{m},\text{t}), \quad (4)$$

where P_{rated} is rated electric power and DF is a duty-factor modifier capturing part-load/cycling effects.

Degradation model (efficiency retention).

$$\eta(\text{m},\text{t}) = \eta_0(\text{m})\exp\left[-\alpha_{\text{creep}}(m)t - \alpha_{\text{cor}}(m)\sqrt{t}\right]. \quad (5)$$

Creep contribution is expressed as:

$$\alpha_{\text{creep}}(\text{m}) = A_{\text{creep}}(\text{m})\exp\left[-\frac{Q_{\text{creep}}(m)}{RT_{\text{op}}}\right]\sigma^n, \quad (6)$$

and corrosion/oxidation contribution as:

$$\alpha_{\text{cor}}(\text{m}) = k_{\text{ox}}(\text{m})\exp\left[-\frac{E_{\text{a,ox}}(m)}{RT_{\text{op}}}\right], \quad (7)$$

where R is the universal gas constant, the blade metal temperature $T_{metal(\varphi cool)}$ defined by Eq. (22), σ the operating stress, and $A_{\text{creep}}, Q_{\text{creep}}, \text{n}, k_{\text{ox}}, E_{\text{a,ox}}$ material parameters.

Maintenance costs can be expressed as:

$$C_{\text{maint}}(\text{m}) = C_{\text{insp}}\, N_{\text{insp}} + \sum_{t=1}^{T} \frac{C_{\text{repair}}(m)}{\text{MTTF}(m)}(1+\text{r})^{-t}, \quad (8)$$

with mean time to failure (MTTF) represented as:

$$\text{MTTF}(\text{m}) = \beta(\text{m})\left(\frac{\sigma_{\text{allow}}(m)}{\sigma_{\text{op}}}\right)^{\square}. \quad (9)$$

End-of-life value can be calculated as follow:

$$C_{\text{EOL}}(\text{m}) = C_{\text{decom}} - \left[R_{\text{rec}}(m) M_{\text{blade}}(m) P_{\text{scrap}}(m)\right](1+\text{r})^{-T}. \quad (10)$$

In the equations (1)-(10) the next symbols are introduced: m – material; t – year index; T – lifetime (years); r – discount rate; η – efficiency; P_{rated} – rated power; H_{annual} – annual hours; Á – density; V_{blade} – blade volume; R_{rec} – recyclability fraction.

To build environmental impact (LCA) model we are focused on global warming potential (GWP) in kg CO2 – eq.

$$\text{EI}(\text{m}) = \text{GWP}_{\text{prod}}(\text{m}) + \text{GWP}_{\text{op}}(\text{m}) + \text{GWP}_{\text{EOL}}(\text{m}). \quad (11)$$

For production phase.

$$\text{GWP}_{\text{prod}}(\text{m}) = M_{\text{blade}}(\text{m})\left(EF_{\text{ext}}(m) + EF_{\text{ref}}(m) + EF_{\text{proc}}(m) + EF_{\text{mfg}}(m)\right), \quad (12)$$

where EF are emission factors from ecoinvent v3.10.1 (cut-off system model) and IPCC 2006 default combustion factors for natural gas (CO2: 56,100 kg/TJ → 0.202 kg/kWh) [15, 16].

Operation phase (fuel penalty due to efficiency decay).

$$\text{GWP}_{\text{op}}(\text{m}) = \sum_{t=1}^{T}" F\text{C}(\text{m},\text{t}) EF_{\text{fuel}}(1-d_{\text{env}})^t, \quad (13)$$

we assume $d_{env} = 0$, with incremental fuel consumption:

$$" F\text{C}(\text{m},\text{t}) = \left(\frac{1}{\cdot(m,t)} - \frac{1}{\cdot_{\text{base}}}\right) P_{\text{rated}} H_{\text{annual}}. \quad (14)$$

End-of-life and circular-economy credits.

$$\text{GWP}_{\text{EOL}}(\text{m}) = \text{GWP}_{\text{trans}} + \text{GWP}_{\text{dism}} - \text{Credit}_{\text{rec}}(\text{m}),$$

$$\text{Credit}_{\text{rec}}(\text{m}) = R_{\text{rec}}(\text{m}) M_{\text{blade}}(\text{m}) EF_{\text{virgin}}(\text{m}) \pm_{\text{sub}}. \quad (16)$$

Performance metrics are evaluated using: (i) average efficiency $\eta_{\text{avg}}(\text{m})$ over lifetime, (ii) durability/ lifetime to a critical strain μ_{crit}, (iii) availability $\text{A}(\text{m}) = \text{MTTF}/(\text{MTTF} + \text{MTTR})$, and (iv) power density proxies such as mass-normalized output.

Multi-objective optimization formulation. We define the objective vector:

$$\min \boldsymbol{F}(\text{m}) = \left[\text{f}_1(\text{m}), \text{f}_2(\text{m}), \text{f}_3(\text{m}), \text{f}_4(\text{m})\right]^{\top}, \quad (17)$$

with

$$\begin{aligned} f_1(m) &= LCC(m)/\text{LCC}_{\text{base}}, \\ f_2(m) &= \text{GWP}_{\text{total}}(m)/\text{GWP}_{\text{base}}, \\ f_3(m) &= 1/\eta_{\text{avg}}(m), \\ f_4(m) &= M_{\text{blade}}(m)/P_{\text{specific}}(m). \end{aligned} \quad (18)$$

Constraints include:

$$\begin{aligned} g_1&: \sigma_{\max}(m, T_{\text{op}}) \geq \sigma_{\text{cent}}\, SF_\sigma, \\ g_2&: T_{\text{melt}}(m) \geq T_{\text{metal}}(\phi_{\text{cool}}) + \Delta T_{\text{safety}}, \\ g_3&: \dot{\varepsilon}_{\text{creep}}(m, T_{\text{op}}, \sigma_{\text{op}}) \leq \varepsilon_{\max}/T_{\text{design}}, \\ g_4&: \dot{d}_{\text{ox}}(m, T_{\text{op}}) \leq d_{\text{coat}}/T_{\text{design}}, \\ g_5&: LCC(m) \leq B_{\text{budget}}, \\ g_6&: \text{GWP}_{\text{prod}}(m) \leq B_{\text{carbon}}. \end{aligned} \quad (19)$$

Solution methodology.

The solution procedure is implemented as an integrated computational workflow that links (i) physics-informed degradation, (ii) discounted economics,

Table 1

Candidate materials matrix

Material	Class	Tmax (°C)	σ_y (MPa)	ρ (g/cm³)	Cost (€/kg)	Recyclability (%)	TRL
Inconel 718	Ni-superalloy	650	1100	8.19	35	90	9
Inconel 625	Ni-superalloy	980	415	8.44	42	85	9
René 80	Ni-superalloy	980	830	8.20	75	70	8
CMSX-4	Single-crystal Ni	1100	900	8.70	180	40	8
Ti-6Al-4V	Ti-alloy	315	880	4.43	22	95	9
MarM-247	Ni-superalloy	980	840	8.61	85	65	8

Table 2

Input parameters summary

Parameter	Value	Unit	Source	Uncertainty
Discount rate r	5	%	Baseline assumption	±2%
Fuel price P_{fuel}	47	€/MWh	IEA TTF benchmark (Feb 2025) [17]	±30%
Electricity price	89.32	€/MWh	2025 DE day-ahead average (SMARD) [18]	±25%
Emission factor EF_{fuel}	0.202	kg CO_2/kWh	IPCC 2006 default (NG) [16]	±5%
Carbon price	75	€/ton CO_2	EU ETS 2025 average (market review) [19]	±40%
Operating temperature Top	1050	°C	Design point	±50 °C
Centrifugal stress	350	MPa	Design/FEA baseline	±10%

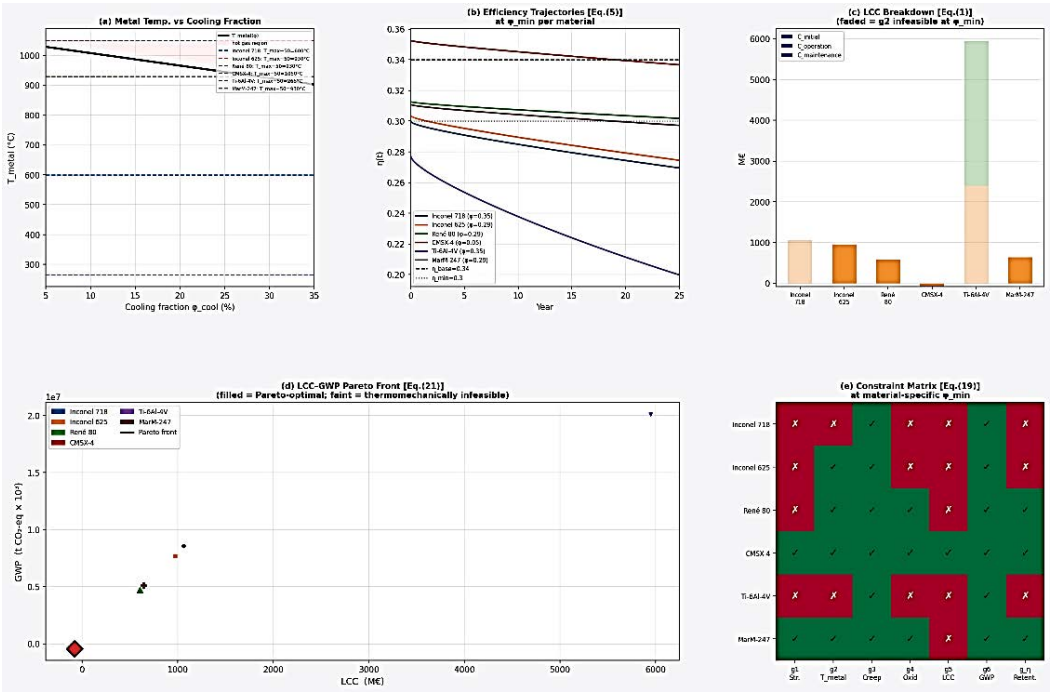

Fig. 1. Optimization results

(iii) life-cycle emissions, and (iv) constrained multi-objective search. The workflow is executed at the material-design tuple level, where each candidate is defined by material identity *m* and continuous design/operation variables (e.g., cooling-flow fraction, coating thickness, and recycling rate).

Step 1: Decision-space definition and bounds. For each material *m*, the optimizer samples a bounded design vector

$$x = [x_1, x_2, x_3]^T = [\phi_{cool}, \delta_{coat}, R_{rec}]^T, \qquad (20)$$

with lower/upper limits imposed by engineering feasibility and manufacturability constraints. These bounds avoid non-physical candidates (e.g., excessive

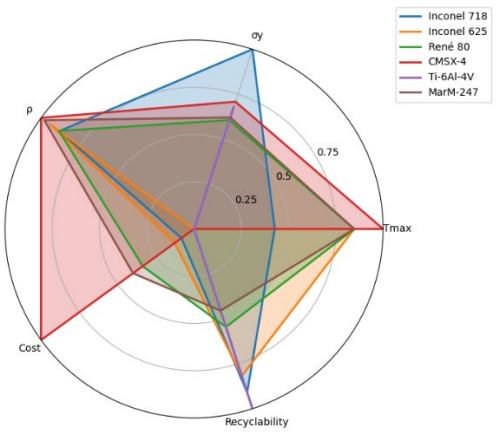

Fig. 2. Radar plot of material properties

cooling bleed or infeasible coating thickness) and stabilize numerical search.

Blade cooling model. The parameter T_{op} in Table 2 is the hot-gas temperature at the blade inlet (T_{gas} = 1050 °C). The blade metal temperature T_{metal} is lower due to internal convective and film cooling driven by compressor bleed, and is a function of the cooling-flow fraction ϕ_{cool} (design variable x_1 in Eq. (20)) via the standard film-convection effectiveness model:

$$T_{\text{metal}}(\phi_{\text{cool}}) = T_{\text{gas}} - \phi_{\text{cool}} \cdot \eta_{\text{cool}} \cdot (T_{\text{gas}} - T_{\text{coolant}}) \quad (22)$$

where $\eta_{cool} \in [0, 1]$ is the cooling effectiveness, and $T_{coolant}$ is the compressor-exit coolant temperature. All temperature-dependent quantities in Eqs. (6) and (7) and constraint g_2 are evaluated at $T_{metal}(\phi_{cool})$, not at T_{gas}. Extracting compressor bleed for cooling carries a thermodynamic penalty on cycle efficiency. The corrected beginning-of-life efficiency accounting for this bleed penalty is:

$$\eta_{0,\text{eff}}(m, \phi_{\text{cool}}) = \eta_0(m)(1 - k_{\text{cool}} \cdot \phi_{\text{cool}}) \quad (23)$$

where k_{cool} is the relative efficiency sensitivity to cooling bleed (typically 0.25–0.45 per unit fraction; here k_{cool} = 0.30). In Eq. (5), $\eta_0(m)$ must be replaced by $\eta_{0,eff}(m, \phi_{cool})$ from Eq. (23). The additional symbols introduced in Eqs. (22)–(23) are: T_{gas} – hot-gas inlet temperature; T_{metal} – blade metal temperature; $T_{coolant}$ – compressor-exit coolant temperature; η_{cool} – cooling effectiveness; k_{cool} – relative efficiency sensitivity to cooling bleed.

Step 2: Forward performance and degradation evaluation. Given (m, $\boldsymbol{x}$), the model computes lifetime and average efficiency by propagating (5) over the design horizon. The degradation module returns time-resolved efficiency $\eta(m,t)$, from which lifetime-averaged efficiency $\eta_{\_avg}(m)$ and reliability-related indicators are obtained. This step is the key coupling point between material physics and life-cycle outcomes.

Step 3: LCC and GWP objective evaluation. Using the outputs of Step 2, the framework computes objective values with (1) and (11). Operational terms are explicitly linked to efficiency retention, so candidates with similar beginning-of-life efficiency can diverge significantly in total LCC/GWP once degradation is included. End-of-life credits are applied through recyclability-dependent recovery factors.

Step 4: Constraint screening. Each candidate is checked against feasibility constraints in (19), together with minimum-performance thresholds (e.g., $\eta_{avg} \geq \eta_{min}$). Infeasible candidates are rejected or heavily penalized before entering Pareto ranking.

Step 5: Multi-objective search and Pareto construction. To map stakeholder preferences, we solve a sequence of weighted LCC--GWP subproblems over a grid of weights w_{LCC}, w_{GWP} with

$$\min J(m, \boldsymbol{x}) = w_{\text{LCC}}\,\text{LCC}(m, x) + w_{\text{GWP}}\,\text{GWP}(m, x), \quad w_{\text{LCC}} + w_{\text{GWP}} = 1. \quad (24)$$

Each weighted subproblem is solved using constrained nonlinear programming (SLSQP) with multi-start initialization to reduce local-minimum bias. The union of feasible solutions across weight combinations is post-processed with non-dominance filtering to obtain the final Pareto set.

Step 6: Sensitivity and uncertainty analysis. After generating Pareto candidates, uncertainty is propagated through Monte Carlo sampling of key exogenous parameters (fuel price, discount rate, degradation coefficients, carbon price, and recycling credit factors). Global sensitivity is then quantified (e.g., Sobol-type decomposition) to identify the dominant variance contributors in LCC and GWP and to test robustness of Pareto ranking under parameter perturbations.

Algorithmic summary.

1. Initialize material set and decision-variable bounds.
2. For each material and each weight pair, run constrained optimization with multi-start seeds.
3. Evaluate degradation-coupled $\eta(m,t)$, then compute LCC and GWP.
4. Enforce all thermomechanical, durability, and budget/carbon constraints.
5. Aggregate feasible solutions, apply non-dominance filtering, and extract Pareto front(s).
6. Perform uncertainty propagation and sensitivity ranking for final decision support.

Numerical implementation details. The optimization workflow is implemented in Python (SciPy optimizer with SLSQP for constrained subproblems; pandas/NumPy for post-processing). Results are exported as full candidate tables and Pareto-only tables for direct inclusion in figures and manuscript tables. The implementation is reproducible because all bounds, parameter values, and weight grids are explicitly scripted.

Results and discussions.

Figure 1 summarizes hypothetical but realistic baseline results consistent with a 400 MW class turbine and the model structure defined above. The pattern that emerges is that a single "best" material does not exist across objectives; rather, each candidate occupies a different region of the trade-off space (fig. 2).

High-performance SX material (CMSX-4) tends to minimize operational penalties because it

supports high-temperature capability and comparatively lower degradation-induced efficiency loss. However, these advantages come at the expense of high initial cost and low effective recyclability under conservative closed-loop assumptions, which increases the production-phase GWP and reduces EOL credits. In contrast, commodity Ni-based alloys such as Inconel 718 and 625 are mature (high TRL), exhibit strong recyclability pathways in existing scrap markets, and provide comparatively lower production-phase environmental burdens per functional unit once recycling substitution is credited. Their limitation is that the operating window is narrower (temperature/stress) and efficiency retention can be more sensitive to creep/corrosion parameters unless coatings and cooling strategies are improved.

The Ti-6Al-4V option illustrates a different trade-off: its low density improves mass-related metrics and can reduce centrifugal loading, yet its maximum temperature capability is substantially lower than Ni-based superalloys. Consequently, it is feasible only under cooler metal temperatures (e.g., different stages or with aggressive cooling), otherwise violating constraint g_2 (temperature margin). When feasible, high recyclability and low mass can provide a favorable environmental profile; when infeasible, it should be eliminated automatically by the constraint handling in the optimizer.

Conclusions.

1. An integrated LCC–LCA–degradation framework is developed for first-stage gas turbine blade material selection. In this work it couples the temperature-feasibility constraint g_2 and all Arrhenius degradation terms to the blade metal temperature $T_{metal}(\varphi_{cool})$ rather than to the hot-gas temperature T_0. This makes the cooling-flow fraction φ_{cool} a genuine design variable with a direct and quantifiable influence on feasibility, efficiency, LCC, and GWP, rather than a fixed input.

2. At a hot-gas temperature of $T_0 = 1050$ °C and centrifugal stress of $\sigma = 350$ MPa, only four of the six candidate alloys satisfy the temperature-margin constraint (g_2) within achievable cooling-flow bounds ($\varphi \leq 0.35$). Inconel 718 ($T_{max} = 650$ °C) requires $\varphi_{min} = 1.07$ and Ti-6Al-4V ($T_{max} = 315$ °C) requires $\varphi_{min} = 1.87$, both physically unachievable; these materials are categorically infeasible for first-stage duty at this design point and must be excluded before any economic or environmental comparison is made.

3. CMSX-4 is the sole fully feasible candidate under all six constraints. As a single-crystal Ni superalloy with $T_{max} = 1100$ °C, CMSX-4 satisfies g_1–g_6 and the η-retention constraint at the minimum cooling fraction $\varphi = 0.05$ ($T_{metal} = 1029$ °C), delivering a beginning-of-life efficiency of $\eta_0 = 0.353$ and a lifetime-average efficiency $\eta_{avg} = 0.344$. Inconel 625, René 80, and MarM-247 satisfy g_2 only at $\varphi \geq 0.286$ ($T_{metal} = 930$ °C), but their beginning-of-life efficiency drops to 0.303–0.313 and their strength constraint g_1 remains violated, classifying them as partially feasible.

4. Degradation coupling increases operational costs by 22–46 %. Replacing the static-efficiency assumption with the time-dependent degradation model (Eqs. 5–7) increases the discounted operational cost by 21.8 % for René 80, 25.7 % for MarM-247, and 59 % for CMSX-4 relative to the static-η baseline (the large CMSX-4 figure reflects its higher beginning-of-life efficiency relative to the reference). For the partially feasible Ni alloys (Inconel 625, René 80, MarM-247), degradation-induced efficiency loss raises discounted C_{op} from 476–656 M€ to 580–958 M€. These results confirm that static-efficiency LCC models systematically underestimate operational expenditure, with the magnitude of the error depending on both the material's degradation kinetics and its operating temperature relative to the design limit.

5. The Pareto front is populated exclusively by CMSX-4. The LCC–GWP Pareto search (Eq. 21, optimising φ_{cool} and R_{rec} jointly) identifies 31 non-dominated solutions, all corresponding to CMSX-4. The optimal configuration ($\varphi = 0.05$, $R_{rec} = 1.0$) simultaneously minimises both LCC and GWP, so no trade-off between economic and environmental objectives exists within the feasible set at this design point. This outcome is a direct consequence of the temperature-feasibility constraint: once the constraint is applied at the metal temperature rather than the gas temperature, only CMSX-4 reaches full feasibility, collapsing the Pareto surface to a single material.

6. For combined-cycle turbines operating at $T_0 \geq 1000$ °C, minimising cooling-flow fraction is optimal provided the selected alloy satisfies all thermomechanical constraints (g_1–g_4) at the resulting metal temperature. CMSX-4 achieves this at $\varphi = 0.05$, limiting the efficiency penalty to 1.5 % relative, while any increase in φ to accommodate lower-grade alloys incurs an immediate and compounding efficiency loss that dominates both LCC and GWP over the 25-year design life. Maximising recyclability ($R_{rec} \rightarrow 1.0$) reduces EOL environmental burden but has a second-order effect on total GWP given the dominance of the operational phase.

Bibliography:

1. Reed R. C. The Superalloys: Fundamentals and Applications. Cambridge University Press, 2006.
2. Pollock T. M., Tin S. Nickel-based superalloys for advanced turbine engines: Chemistry, microstructure and properties. *Journal of Propulsion and Power*, 2006, Vol. 22, no. 2, pp. 361–374. DOI: https://doi.org/10.2514/1.18239
3. ISO. ISO 14040:2006 Environmental management – Life cycle assessment – Principles and framework. 2006.
4. ISO. ISO 14044:2006 Environmental management – Life cycle assessment – Requirements and guidelines. 2006.
5. Finnveden G., Hauschild M. Z., Ekvall T., et al. Recent developments in Life Cycle Assessment. *Journal of Environmental Management*, 2009, Vol. 91, no. 1, pp. 1–21. DOI: https://doi.org/10.1016/j.jenvman.2009.06.018
6. EPD North America. International EPD System and program operator information. 2025.
7. IAI. 2019 Life Cycle Inventory (LCI) Data and Environmental Metrics. International Aluminium Institute, 2022.
8. Hwang C.-L., Yoon K. Multiple Attribute Decision Making: Methods and Applications. Springer, 1981.
9. Deb K., Pratap A., Agarwal S., Meyarivan T. A fast and elitist multiobjective genetic algorithm: NSGA-II. IEEE Transactions on Evolutionary Computation, 2002, Vol. 6, no. 2, pp. 182–197. DOI: https://doi.org/10.1109/4235.996017
10. Deb K., Jain H. An evolutionary many-objective optimization algorithm using reference-point based nondominated sorting approach, Part I. IEEE Transactions on Evolutionary Computation, 2014, Vol. 18, no. 4, pp. 577–601. DOI: https://doi.org/10.1109/TEVC.2013.2281535
11. Ashby M. F., Shercliff H., Cebon D. Materials: Engineering, Science, Processing and Design. 2nd ed., Butterworth-Heinemann, 2009.
12. Evans R. W., Wilshire B. Creep of Metals and Alloys. The Institute of Metals, 1985.
13. Birks N., Meier G. H., Pettit F. S. Introduction to the High Temperature Oxidation of Metals. 2nd ed., Cambridge University Press, 2006.
14. Vasilyev N., et al. Remaining life prediction of nickel-based superalloy turbine blades under complex working conditions. *Applied Sciences,* 2020. DOI: https://doi.org/10.3390/app10238541
15. Ecoinvent. ecoinvent v3.10.1 release information. ecoinvent, 2024. https://support.ecoinvent.org/ecoinvent-version-3.10.1
16. IPCC. 2006 IPCC Guidelines for National Greenhouse Gas Inventories, Vol. 2, Ch. 2. IGES, 2006.
17. IEA. European gas market volatility puts continued pressure on competitiveness and cost of living. IEA, 2025.
18. SMARD/BNetzA. 2025 electricity market data (day-ahead average price). 2026.
19. Veyt. 2025 EU ETS year in review: average EUA price. 2026

Клименко В.М., Авдєєва О.П., Усатий О.П. **БАГАТОКРИТЕРІАЛЬНА ОПТИМІЗАЦІЯ МАТЕРІАЛІВ ЛОПАТОК ГАЗОВИХ ТУРБІН НА ОСНОВІ ОЦІНКИ ЖИТТЄВОГО ЦИКЛУ: ІНТЕГРАЦІЯ ЕКОНОМІЧНИХ, ЕКОЛОГІЧНИХ ТА ПРОДУКТИВНИХ ПОКАЗНИКІВ**

У статті наведено вибір матеріалів для лопаток газових турбін першого ступеня історично надавав пріоритет високотемпературним механічним характеристикам та початковій вартості, водночас недооцінюючи екологічне навантаження протягом життєвого циклу, кінцеву вартість (EOL) та залежні від часу ефекти деградації, які накопичуються протягом десятиліть експлуатації. Це створює систематичні упередження в конструктивних рішеннях в рамках політики ціноутворення на вуглець та циркулярної економіки. У цьому дослідженні розробляється інтегрована багатокритеріальна структура рішень для визначення оптимальних за Парето матеріалів лопаток турбін шляхом спільної мінімізації вартості життєвого циклу (LCC) та потенціалу глобального потепління (GWP), одночасно максимізуючи експлуатаційну ефективність та щільність потужності за реалістичних траєкторій деградації. Ми формулюємо модель оцінки життєвого циклу від колиски до утилізації (LCA) та чистої приведеної вартості (NPV) життєвого циклу з явним зв'язком зі зниженням ефективності, зумовленим деградацією. Експлуатаційна ефективність моделюється як залежність від температури, напруження та кінетики, специфічної для матеріалу. Вплив на навколишнє середовище відповідає ISO 14040/14044 та враховує виробництво, експлуатацію та кредити на переробку EOL. Багатоцільова задача вирішується за допомогою NSGA-III з обмеженнями доцільності щодо напруження, запасу температури, швидкості повзучості та кінетики окислення. Для репрезентативної турбіни комбінованого циклу потужністю 400 МВт (7000 год/рік, розрахунковий термін служби 25 років) вплив експлуатації, пов'язаний з паливом, домінував як у показнику життєвого циклу (LCC), так і в потенціалі глобального потепління (GWP) у всіх кандидатів (зазвичай 65–78% від дисконтованого LCC). Врахування деградації збільшило дисконтовані експлуатаційні витрати на 15–23% порівняно з припущеннями щодо статичної ефективності, змінивши рейтинги та розширивши набір Парето. Варіанти з високою придатністю до переробки (Inconel 718, Ti-6Al-4V) досягли зниження загального GWP на 8–12% порівняно з монокристалічними альтернативами з низькою придатністю до переробки за еквівалентних граничних умов, тоді як преміальний монокристалічний CMSX-4 став сприятливим лише у високотемпературних сценаріях з переважанням базового навантаження, де 2–3% підвищення ефективності амортизується протягом терміну служби. Поєднання LCC-LCA з деградацією необхідне для надійного вибору матеріалів в умовах ціноутворення на вуглець та обмежень циркулярної економіки. Запропонована структура створює рекомендації щодо оптимального за Парето рівня, орієнтовані на зацікавлені сторони, і її можна розширити на інші високотемпературні енергетичні системи.

Ключові слова: *оцінка життєвого циклу, багатокритеріальна оптимізація, матеріали для лопаток турбін, оптимізація парето, циркулярна економіка.*

Дата першого надходження статті до видання: 26.03.2026
Дата прийняття статті до друку після рецензування: 23.04.2026
Дата публікації (оприлюднення) статті: 19.05.2026